

# 1 The molecular pathogenesis of the *NUP98-HOXA9* fusion protein in Acute 2 Myeloid Leukemia

3 Ana Rio-Machin <sup>1,2</sup>; Gonzalo Gomez-Lopez <sup>3</sup>; Javier Muñoz <sup>4</sup>; Fernando Garcia-Martinez <sup>4</sup>; Alba  
4 Maiques-Diaz <sup>1</sup>; Sara Alvarez <sup>1</sup>; Rocio N Salgado <sup>1</sup>; Mahesh Shrestha <sup>5</sup>; Raúl Torres <sup>6</sup>; Claudia Haferlach  
5 <sup>7</sup>; Maria Jose Larrayoz <sup>8</sup>; Maria Jose Calasanz <sup>8</sup>; Jude Fitzgibbon <sup>2</sup> and Juan C. Cigudosa <sup>1</sup>

6 <sup>1</sup> Molecular Cytogenetics Group, Human Cancer Genetics Programme, Centro Nacional Investigaciones  
7 Oncologicas (CNIO), Madrid, Spain

8 <sup>2</sup> Centre for Haemato-Oncology, Barts Cancer Institute, Queen Mary University of London, UK

9 <sup>3</sup> Bioinformatics Unit, Centro Nacional Investigaciones Oncologicas (CNIO), Madrid, Spain

10 <sup>4</sup> Proteomics Unit, Centro Nacional Investigaciones Oncologicas (CNIO), Madrid, Spain. ProteoRed-ISCIII.

11 <sup>5</sup> Division of Experimental Hematology and Cancer Biology, Cincinnati Children's Hospital Medical Center,  
12 Cincinnati, OH, USA

13 <sup>6</sup> Viral Vector Facility, Fundacion Centro Nacional de Investigaciones Cardiovasculares (CNIC), Madrid, Spain

14 <sup>7</sup> MLL Münchner Leukämie Labor, München, Germany

15 <sup>8</sup> Department of Genetics and Center for Applied Medical Research (CIMA), University of Navarra, Pamplona,  
16 Spain

17

## 18 Corresponding author:

19 **Ana Rio-Machin, PhD**

20 Centre for Haemato-Oncology

21 Barts Cancer Institute

22 Queen Mary University of London

23 John Vane Science Centre, Charterhouse Square,

24 London EC1M 6BQ (United Kingdom)

25 Tel: +44 (0)20 7882 8780

26 Email: [a.rio-machin@qmul.ac.uk](mailto:a.rio-machin@qmul.ac.uk)

27

## 28 DISCLOSURE OF CONFLICTS OF INTEREST

29 The authors have declared that no conflict of interest exists.

30

31 Recurrent chromosomal translocations are common initiation events and have provided  
32 important insights into the pathogenesis of AML, paving the way for the introduction of novel targeted  
33 therapies. However, clinical outcomes, in particular for patients with adverse cytogenetic features  
34 remain suboptimal. The chromosomal translocation t(7;11)(p15, p15), encoding the fusion protein  
35 NUP98-HOXA9 (NHA9), is a rare poor risk cytogenetic event in AML associated with a particularly poor  
36 prognosis. NHA9 brings the FG repeat-rich portion of the nucleoporin NUP98 upstream of the  
37 homeodomain and *PBX* heterodimerization domains of HOXA9, and acts as oncogenic transcription  
38 factor <sup>1</sup>. The pathogenic events underlying NHA9 remain poorly understood and herein, we aim to  
39 characterize the downstream mediators of this oncoprotein by determining the effects of the fusion  
40 using human cellular models.

41 We set out initially to compare the DNA binding sites of *NHA9*, *HOXA9* and *NUP98*, by forced  
42 expression of these genes alone or the corresponding fusion gene by retroviral transduction of  
43 HEK93FT cell line and cord blood-isolated human hematopoietic progenitors (hHP). ChIP-seq analysis  
44 in the HEK293FT cellular model identified 4 471 significant genomic regions (false discovery rate (FDR)  
45 < 0.05) as target sites of the fusion protein, all located within -5/+ kb from the annotated Transcription  
46 Start Site (TSS) (Figure S1A). They correspond to 1 368 genes and 17 miRNAs (Table S1) of which 399  
47 genes were also shown to be common targets of *HOXA9* and 4 of *NUP98* (Figure 1A, Table S2, Figures  
48 S1C-D) [See supplementary methods] (Data deposited in GEO <http://www.ncbi.nlm.nih.gov/geo/>,  
49 accession number: GSE62587). Ingenuity pathway analysis of the NHA9 target series demonstrated a  
50 significant enrichment of pathways associated with tumorigenesis and leukemic differentiation  
51 (Figure S1B).

52 We next performed a detailed sequence analysis of the NHA9 binding sites using the MEME-ChIP  
53 algorithm and detected a significant overlap with binding of several HOX genes, including *HOXA9*,  
54 supporting a role for this homeodomain in the DNA binding of NHA9. Strikingly, NHA9 sites were  
55 enriched for a novel binding motif, CA/gTTT, that was present in one-third (n = 1 421) of all NHA9 ChIP-  
56 seq regions (Table S3). This motif had not been previously associated with any known transcription

57 factor and was not observed in wild type *HOXA9* or *NUP98* binding site experiments, suggesting that  
58 it is specific to NHA9 DNA binding. MEME-ChIP (SpaMO) was used to identify significant co-  
59 occurrences of other known DNA binding motifs with this novel NHA9 DNA binding motif. Binding  
60 motifs corresponding to 12 transcription factors, including other HOX family proteins such as HOXB7  
61 or HOXD11, were found to be overrepresented within the region adjacent to CA/gTTT (Table S4),  
62 suggesting a possible functional cooperation with the fusion oncoprotein.

63 As the NHA9 target motifs are preferentially located more than 1 kb upstream/downstream of  
64 the TSS (Figure S1A), we reasoned that NHA9 binding may coincide with particular enhancer elements.  
65 A similar distribution was also found for the identified *HOXA9* target regions whereas *NUP98* binding  
66 sites were mostly located within promoters, both in agreement with previous studies <sup>2,3</sup>. We selected  
67 eight leukemia-related genes (*MEIS1*, *HOXA9*, *PBX3*, *MET*, *BRAF*, *AF9*, *PTEN* and *NF1*) identified as part  
68 of our NHA9 ChIP-seq experiments, for locus specific qChIP studies. A significant enrichment of  
69 H3K4me1, a chromatin mark that predicts poised and active enhancers, and RNA Polymerase II (PolII),  
70 which is consistent with the presence of the active form of the enhancers <sup>4,5</sup>, was shown within the  
71 NHA9 binding sites upstream of the eight genes (Figures 1B and S1E). NHA9 expression levels were  
72 demonstrated to be comparable in our two cellular models (HEK293FT and hHP) (Figure S1G).  
73 Accordingly, we validated the ChIP-seq results in the HEK293FT model (Figure S1F) using the same set  
74 of eight NHA9 target genes and also demonstrated binding of NHA9 to the eight enhancers in our  
75 second model system of NHA9-expressing hHP cells (Figure 1C), allowing us to confirm these findings  
76 in primary human hematopoiesis.

77 We next focused attention on the transcription factors *MEIS1*, *HOXA9* and *PBX3*, as their  
78 overexpression is significantly related to adverse prognosis in AML (The Cancer Genome Atlas <sup>6</sup>; Figure  
79 S1H) and were previously reported to drive leukemogenesis through the formation of a transcriptional  
80 activator complex <sup>7</sup>. To test the importance of these three transcription factors in NHA9 pathogenesis,  
81 we completed reporter assays in HEK293FT cells by cloning the identified enhancers of *MEIS1*, *HOXA9*  
82 or *PBX3* into a luciferase reporter vector. A significant 1.6-2.8 fold induction in luciferase activity was

83 observed when NHA9 was co-expressed for all three enhancers, indicating a direct induction of *MEIS1*,  
84 *HOXA9* and *PBX3* expression through the NHA9 interaction with their corresponding regulatory  
85 regions (Figure 1D) [see Supplementary Methods]. This observation was accompanied by upregulation  
86 of all 3 transcription factors and of three of their known target genes (*MYB*, *MEF2C* and *FLT3*)<sup>7</sup> in  
87 NHA9-expressing hHP cells (Figure 1E and S1I). Gene Expression Profiling performed in three  
88 independent NHA9-expressing hHP clones and AMLs from 5 patients with t(7;11)(p15,p15), confirmed  
89 *MEIS1-HOXA9-PBX3* overexpression and it was further validated by RT-qPCR analysis in 3 additional  
90 NHA9 primary samples (Figure S2A). These observations suggested that the NHA9-expressing hHP cells  
91 can be sensitive to HXR9, a specific peptide inhibitor of HOXA9 and PBX3 interaction that leads to  
92 disruption of the MEIS1-HOXA9-PBX3<sup>8</sup> complex. We tested this hypothesis by treating these cells with  
93 HXR9 that resulted in a selective decrease in their viability (Figure 1F and S2B-D) [see Supplementary  
94 Methods] without affecting cell differentiation (data not shown), therefore confirming the relevance  
95 of these downstream mediators in driving the oncogenic activity of NHA9.

96 In order to explore other mechanisms driving NHA9 pathogenesis and to better understand its  
97 role in transcriptional regulation, we interrogated our ChIP-seq and gene expression profiling data,  
98 which revealed both activation and repression of gene expression induced by this fusion oncoprotein  
99 (Figure 2A). The cooperation of MLL1 and CRM1 with NHA9 in the upregulation of some target genes  
100 has been shown recently by Xu *et al.*<sup>9,10</sup>, which was also supported by comparing NHA9 target genes  
101 identified in our ChIP-seq experiments with MLL1 and CRM1 targets. We found that 25% and 35% of  
102 NHA9 target genes were also in common with MLL1 and CRM1 target genes, respectively (Figure S2E).  
103 Notably, 151 target genes, including *MEIS1* and *HOXA9*, were shared by all three proteins (NHA9, MLL1  
104 and CRM1), suggesting a possible cooperation among these transcription factors in NHA9-driven  
105 leukemias. It has also been reported that NUP98, through its FG repeat domain, may interact with  
106 transcriptional activator p300 and repressor HDACs<sup>11</sup>, allowing us to postulate that transcriptional  
107 effects of NHA9 in enhancers could be mediated by these regulators. We first demonstrated NHA9  
108 binding to both p300 and HDAC1 by Co-immunoprecipitation experiments (Figure 2B) [see

109 Supplementary Methods] and went on to examine their binding potential in a panel of eight regulatory  
110 regions of NHA9 target genes (four upregulated and four downregulated target genes) in the presence  
111 of the fusion protein by qChIP. These experiments demonstrated selective binding of p300 to the  
112 regulatory regions of the upregulated genes *MEIS1*, *HOXA9*, *PBX3* and *AFF3* (Figure 2C), and of HDAC1  
113 to the downregulated genes *BIRC3*, *SMAD1*, *FILIP1L* and *PTEN* (Figure 2D). Altogether this data  
114 suggests that p300 and HDAC1 are selectively recruited by NHA9 at enhancer regions to modulate the  
115 expression of genes involved in leukemogenesis.

116 As the interaction of NHA9 with HDAC1/2 was validated by mass spectrometry analysis using the  
117 NHA9-expressing HEK293FT model (Proteomics data have been deposited on the ProteomeXchange  
118 Consortium via the PRIDE partner repository, data set identifier PXD001828)) [see Supplementary  
119 Methods], we had a molecular rationale for testing HDAC inhibitors (HDACi) in NHA9 AML. We  
120 assessed the sensitivity of the hHP-NHA9 model to the pan-HDACi LBH589 (Panobinostat) and  
121 observed a strong inhibitory effect that was significantly higher ( $IC_{50_{hHP-NHA9}} \approx 4nM$ ) than its inhibitory  
122 effect in MLL-AF9 -expressing ( $IC_{50_{hHP-MLL\_AF9}} \approx 30nM$ ) or AML1-ETO-expressing ( $IC_{50_{hHP-AML1\_ETO}} \approx 200nM$ ) hHP cells<sup>12, 13</sup>, where the efficacy of this component has been already established<sup>14</sup>,  
123 <sup>15</sup> (Figure 2E). Accordingly, treatment with low doses (4nM) of LBH589 completely abrogated the  
124 ability of hHP-NHA9 cells to form colonies in the CFC assay (Figure S2F) and significantly induced  
125 apoptosis within 24h (4nM and 30nM doses), whereas LBH589 had no effect at the same doses on the  
126 empty vector control hHP cells (Figure S2G). It has to be noted that LBH589 did not induce  
127 differentiation in NHA9-expressing cells as no significant changes in the number of CD11b positive  
128 cells were observed by flow cytometry analysis post treatment (data not shown). These observations  
129 are in accordance with a recent report suggesting the combination of COX or DNMT inhibitors with  
130 HDACi for treatment of NHA9 AML patients<sup>16</sup>, however in this study we identified the molecular  
131 rationale for HDACi therapy as well as a panel of target genes downstream of NHA9 that can be used  
132 as biomarkers for response to this treatment. Furthermore, our hHP-NH9A cellular model showed  
133 sensitivity to markedly lower concentrations of LBH589 (4nM) than the recommended doses in  
134

135 preclinical studies and Multiple Myeloma Clinical Trials <sup>17, 18</sup>, indicating that LBH589 could be safely  
136 used as novel targeted therapy for the treatment of NH9A AML patients. However, the biological  
137 consequences of this therapy, as well as the best dosage-time relation for the translation into clinics  
138 need to be further investigated.

139 In summary, NHA9 deregulates the expression of key leukemic genes, including *MEIS1-HOXA9-*  
140 *PBX3* complex, through the enhancer binding and the direct interaction of the fusion protein with  
141 HDAC and p300 transcriptional regulators. The oncogenic effects of NHA9 can be overcome by HDACi  
142 treatment, demonstrating a significant inhibitory effects against NHA9-driven leukemic cells and  
143 suggesting a novel approach to treatment of this high-risk group of patients.

144

145

146 **Supplementary information is available at Leukemia's website**

147 (<http://www.nature.com/leu/index.html>)

148

149

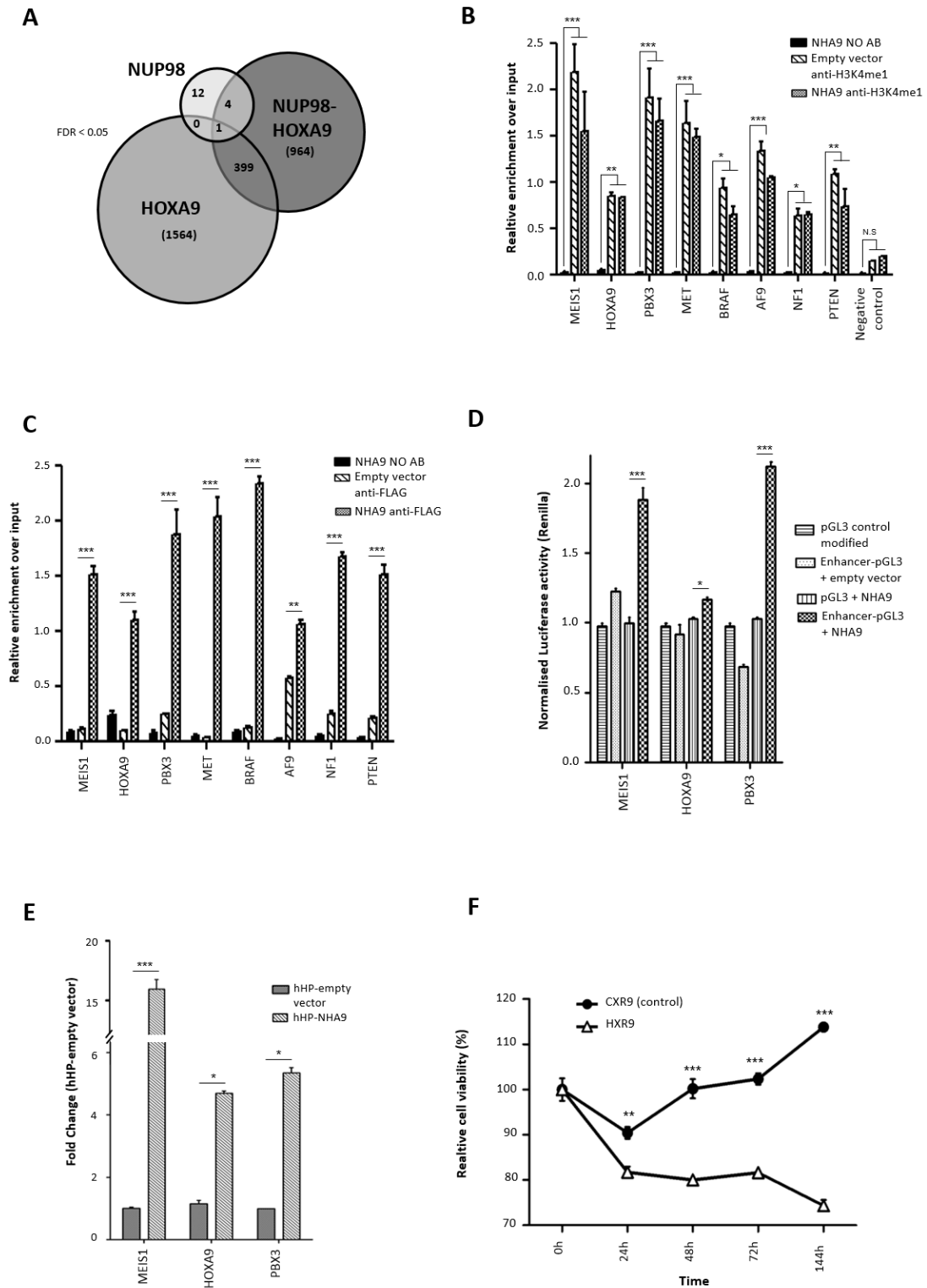
## 150 REFERENCES

151

152

- 153 1. Takeda A, Goolsby C, Yaseen NR. NUP98-HOXA9 induces long-term proliferation and blocks  
154 differentiation of primary human CD34+ hematopoietic cells. *Cancer research* 2006 Jul 1;  
155 **66**(13): 6628-6637.
- 156 2. Huang Y, Sitwala K, Bronstein J, Sanders D, Dandekar M, Collins C, *et al.* Identification and  
157 characterization of Hoxa9 binding sites in hematopoietic cells. *Blood* 2012 Jan 12; **119**(2): 388-  
158 398.
- 159 3. Liang Y, Franks TM, Marchetto MC, Gage FH, Hetzer MW. Dynamic association of NUP98 with  
160 the human genome. *PLoS genetics* 2013; **9**(2): e1003308.
- 161 4. Smith E, Shilatifard A. Enhancer biology and enhanceropathies. *Nature structural & molecular*  
162 *biology* 2014 Mar; **21**(3): 210-219.
- 163 5. De Santa F, Barozzi I, Mietton F, Ghisletti S, Polletti S, Tusi BK, *et al.* A large fraction of  
164 extragenic RNA pol II transcription sites overlap enhancers. *PLoS biology* 2010 May; **8**(5):  
165 e1000384.
- 166
- 167
- 168
- 169

- 170  
171 6. Cancer Genome Atlas Research N. Genomic and epigenomic landscapes of adult de novo acute  
172 myeloid leukemia. *The New England journal of medicine* 2013 May 30; **368**(22): 2059-2074.  
173  
174 7. Garcia-Cuellar MP, Steger J, Fuller E, Hetzner K, Slany RK. Pbx3 and Meis1 cooperate through  
175 multiple mechanisms to support Hox-induced murine leukemia. *Haematologica* 2015 Jul;  
176 **100**(7): 905-913.  
177  
178 8. Li Z, Zhang Z, Li Y, Arnovitz S, Chen P, Huang H, *et al.* PBX3 is an important cofactor of HOXA9  
179 in leukemogenesis. *Blood* 2013 Feb 21; **121**(8): 1422-1431.  
180  
181 9. Xu H, Valerio DG, Eisold ME, Sinha A, Koche RP, Hu W, *et al.* NUP98 Fusion Proteins Interact  
182 with the NSL and MLL1 Complexes to Drive Leukemogenesis. *Cancer cell* 2016 Dec 12; **30**(6):  
183 863-878.  
184  
185 10. Oka M, Mura S, Yamada K, Sangel P, Hirata S, Maehara K, *et al.* Chromatin-prebound Crm1  
186 recruits Nup98-HoxA9 fusion to induce aberrant expression of Hox cluster genes. *eLife* 2016  
187 Jan 07; **5**: e09540.  
188  
189 11. Moore MA, Chung KY, Plasilova M, Schuringa JJ, Shieh JH, Zhou P, *et al.* NUP98 dysregulation  
190 in myeloid leukemogenesis. *Annals of the New York Academy of Sciences* 2007 Jun; **1106**: 114-  
191 142.  
192  
193 12. Wei J, Wunderlich M, Fox C, Alvarez S, Cigudosa JC, Wilhelm JS, *et al.* Microenvironment  
194 determines lineage fate in a human model of MLL-AF9 leukemia. *Cancer cell* 2008 Jun; **13**(6):  
195 483-495.  
196  
197 13. Mulloy JC, Cammenga J, Berguido FJ, Wu K, Zhou P, Comenzo RL, *et al.* Maintaining the self-  
198 renewal and differentiation potential of human CD34+ hematopoietic cells using a single  
199 genetic element. *Blood* 2003 Dec 15; **102**(13): 4369-4376.  
200  
201 14. Bots M, Verbrugge I, Martin BP, Salmon JM, Ghisi M, Baker A, *et al.* Differentiation therapy for  
202 the treatment of t(8;21) acute myeloid leukemia using histone deacetylase inhibitors. *Blood*  
203 2014 Feb 27; **123**(9): 1341-1352.  
204  
205 15. Baker A, Gregory GP, Verbrugge I, Kats L, Hilton JJ, Vidacs E, *et al.* The CDK9 Inhibitor Dinaciclib  
206 Exerts Potent Apoptotic and Antitumor Effects in Preclinical Models of MLL-Rearranged Acute  
207 Myeloid Leukemia. *Cancer research* 2016 Mar 1; **76**(5): 1158-1169.  
208  
209 16. Deveau AP, Forrester AM, Coombs AJ, Wagner GS, Grabher C, Chute IC, *et al.* Epigenetic  
210 therapy restores normal hematopoiesis in a zebrafish model of NUP98-HOXA9-induced  
211 myeloid disease. *Leukemia* 2015 Oct; **29**(10): 2086-2097.  
212  
213 17. Anne M, Sammartino D, Barginear MF, Budman D. Profile of panobinostat and its potential for  
214 treatment in solid tumors: an update. *OncoTargets and therapy* 2013; **6**: 1613-1624.  
215  
216 18. San-Miguel JF, Hungria VT, Yoon SS, Beksac M, Dimopoulos MA, Elghandour A, *et al.*  
217 Panobinostat plus bortezomib and dexamethasone versus placebo plus bortezomib and  
218 dexamethasone in patients with relapsed or relapsed and refractory multiple myeloma: a  
219 multicentre, randomised, double-blind phase 3 trial. *The Lancet Oncology* 2014 Oct; **15**(11):  
220 1195-1206.



222 **Figure 1: NUP98-HOXA9 binds to enhancers of genes related to leukemogenesis (A)** Venn diagrams  
 223 of NHA9, HOXA9 and NUP98 target genes identified by ChIP-seq experiments on HEK293FT human  
 224 models and located within +5/-5 kb of an annotated Transcription Start Site (TSS). Significant ChIP-seq  
 225  
 226

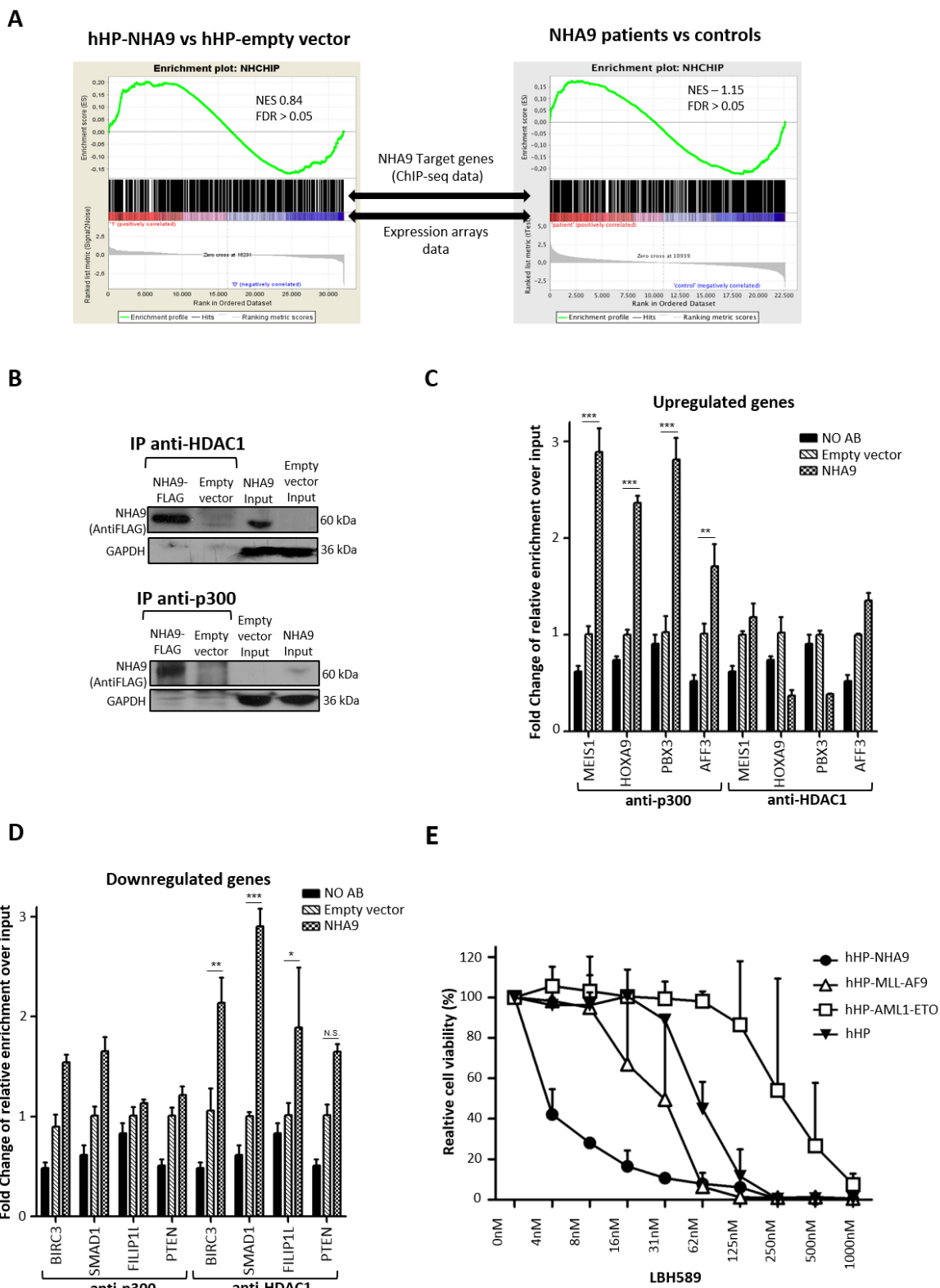


227 peaks were established at  $FDR \leq 5\%$ . **(B)** H3K4me1 qChIP fold enrichment in the selected NHA9 target  
228 regions using anti-H3K4me1 antibody. The MEIS1 promoter region was used as a negative control. The  
229 average of three experiments is shown. Error bars represent SEM. **(C)** NHA9 qChIP fold enrichment on  
230 the eight selected NHA9 target enhancer regions using *anti-FLAG* antibody in the NHA9 expressing  
231 hHP cellular model. The average of 3 experiments is shown. Error bars represent SEM. **(D)** Luciferase  
232 assay was performed to analyze the role of NHA9 in regulating the expression of *HOXA9*, *PBX3* and  
233 *MEIS1*. The luciferase constructs containing the enhancer region (using *pGL3-Promoter* vector,  
234 Promega Biotech Ibérica S.L) of *HOXA9*, *PBX3* and *MEIS1* were co-transfected into HEK293FT cells with  
235 the expression vector pMSCV-NHA9, together with Renilla vector for the purpose of normalization.  
236 Luciferase activity was determined 48 h after reporter plasmid transfection in all cases. A significant  
237 increase in luciferase activity induced by NHA9 expression was observed in each case, confirming a  
238 direct increase of *MEIS1*, *HOXA9* and *PBX3* expression through NHA9 interaction with their  
239 corresponding enhancer regions. Data are presented as the mean value from two separate  
240 experiments with  $n=3$  for each experiment. Error bars represent SEM. **(E)** Expression analysis by qRT-  
241 PCR of *MEIS1*, *HOXA9* and *PBX3* in the NHA9 expressing hHP cellular model. The expression of the  
242 endogenous human housekeeping gene GAPDH was used to normalize the data, which are expressed  
243 as the mean of  $2^{-\Delta Ct}$  values obtained for each sample after normalization based on the hHP-empty  
244 vector model. **(F)** Analysis of the hHP-NHA9 response to HXR9 and CXR9 (control) peptides. hHP-NHA9  
245 cells were plated in 96-well plates in triplicate and exposed to 13uM of HXR9/CXR9. Cell viability was  
246 assessed at different time points. Average normalized optical density (OD) values of three  
247 independent experiments are shown.

248 Statistical significance for relative enrichment and proliferation was determined at  $p < 0.05$  (\*),  $p <$   
249  $0.01$  (\*\*) and  $p < 0.001$  (\*\*\*), using a t-test with Bonferroni correction. N.S corresponds to non-  
250 significant comparisons. Error bars represent SEM.

251

252



254

255 **Figure 2: NUP98-HOXA9 has an activator-repressor role in transcriptional regulation driven by *p300***

256 **and *HDAC1* interactions. (A)** We applied gene set enrichment analysis (GSEA) to test for enrichment

257 of NHA9 ChIP-seq target gene set among differentially expressed genes using expression array data  
258 from hHP-NHA9 cellular model (left panel) and five NHA9 primary samples (right panel). Genes were  
259 ranked based on the limma-moderated t statistic. After Kolmogorov-Smirnoff testing, those gene sets  
260 with FDR <0.25, a well-established cut-off for the identification of biologically relevant gene sets, were  
261 considered enriched **(B)** Analysis of NHA9 and p300/HDAC1 interactions by co-immunoprecipitation.  
262 HEK293FT cells were transfected with pMSCV-NUP98-HOXA9 or pMSCV-empty vectors. 48h post-  
263 transfection, the immunoprecipitation was performed using *anti-p300* and *anti-HDAC1* antibodies  
264 and the proteins were analyze by immunoblotting using *anti-FLAG* antibody. Endogenous *GAPDH*  
265 protein levels were used as a loading control. **(C & D)** qChIP fold enrichment of p300 and HDAC1 in  
266 the regulatory regions of four upregulated (C) and four downregulated (D) target genes of NHA9. The  
267 average of 3 experiments showed the binding, along with the fusion protein, of p300 and HDAC1 to  
268 the regulatory regions of the overexpressed and downregulated NHA9-target genes, respectively. **(E)**  
269 Analysis of the hHP-NHA9 response to HDAC inhibitors. Cells were exposed for 72 hours to serial  
270 dilutions of panobinostat (LBH589) followed by the addition of WST-1 to assess cell viability. The  
271 average normalized optical density (OD) values are shown compared to vehicle.  
272 Statistical significance for relative enrichment and proliferation was determined at  $p < 0.05$  (\*),  $p <$   
273  $0.01$  (\*\*) and  $p < 0.001$  (\*\*\*), using a t-test with Bonferroni correction. N.S corresponds to non-  
274 significant comparisons. Error bars represent SEM.  
275